HHS Public Access

Author manuscript

Exp Eye Res. Author manuscript; available in PMC 2018 January 01.

Published in final edited form as:

Exp Eye Res. 2017 January ; 154: 70–78. doi:10.1016/j.exer.2016.11.008.

Spatial distributions of glutathione and its endogenous conjugates in normal bovine lens and a model of lens aging

Mitchell G. Nye-Wood[1], **Jeffrey M. Spraggins**[2,3,4], **Richard M. Caprioli**[2,3,4], **Kevin L. Schey**[2,3,5], **Paul J. Donaldson**[1], and **Angus C. Grey**[1]

[1]School of Medical Sciences, University of Auckland, Auckland, New Zealand [2]Mass Spectrometry Research Centre, Vanderbilt University, Nashville, TN, USA [3]Department of Biochemistry, Vanderbilt University, Nashville, TN, USA [4]Department of Chemistry, Vanderbilt University, Nashville, TN, USA [5]Department of Ophthalmology and Visual Sciences, Vanderbilt University, Nashville, TN, USA

Abstract

Glutathione (GSH) is the archetypal antioxidant, and plays a central role in the protection of the ocular lens from cataract formation. High levels of GSH are maintained in the transparent lens, but with advancing age, GSH levels fall in the lens nucleus relative to outer cortical cells, thereby exposing the nucleus of the lens to the damaging effects of oxygen radicals, which ultimately leads to age-related nuclear (ARN) cataract. Under normal conditions, GSH also forms endogenous conjugates to detoxify the lens of reactive cellular metabolites and to maintain cell homeostasis. Due to the intrinsic gradient of lens fibre cell age, the lens contains distinct regions with different metabolic requirements for GSH. To investigate the impact of fibre cell and lens aging on the varied roles that GSH plays in the lens, we have utilised high mass resolution MALDI mass spectrometry profiling and imaging analysis of lens tissue sections. High Dynamic Range (HDR)-MALDI FTICR mass spectrometry was used as an initial screening method to detect regional differences in lens metabolites from normal bovine lenses and in those subjected to hyperbaric oxygen as a model of lens aging. Subsequent MALDI imaging analysis was used to spatially map GSH and its endogenous conjugates throughout all lenses. Accurate mass measurement by MALDI FTICR analysis and LC-MS/MS mass spectrometry of lens region homogenates were subsequently used to identify endogenous GSH conjugates. While the distribution and relative abundance of GSH-related metabolic intermediates involved in detoxification pathways remained relatively unchanged upon HBO treatment, those involved in its antioxidant function were altered under conditions of oxidative stress. For example, reduced glutathione levels were decreased in the lens cortex while oxidised glutathione levels were elevated in the lens outer cortex upon HBO treatment. Interestingly, cysteineglutathione disulfide, was detected in the inner cortex of the normal lens, but was greatly decreased in the HBO-treated lenses. These results contribute to our

Corresponding Author: Angus C. Grey, PhD, Department of Physiology, School of Medical Sciences, University of Auckland, ac.grey@auckland.ac.nz, Ph: +64 9 9233174.

understanding of the multiple roles that GSH plays in maintenance of lens transparency and in the age-related metabolic changes that lead to lens cataract formation.

Graphical Abstract

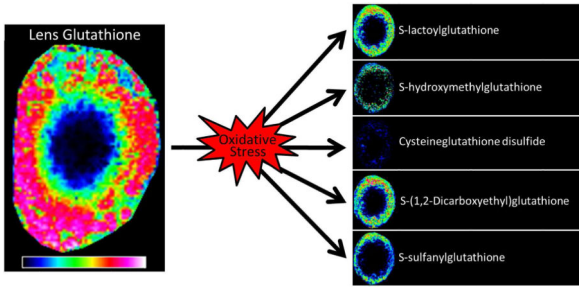

Keywords

Glutathione; MALDI imaging; cataract; lens; HDR mass spectrometry; FTICR Mass Spectrometry

1. INTRODUCTION

The ocular lens is a unique structure that focusses light onto the retina in order to form a sharp image. The lens has several adaptations to do this effectively. It is avascular, has an ordered cellular structure, and loses light scattering cellular organelles as lens fibre cells mature (Bassnett, 1995; Bassnett and Beebe, 1992). Since it is a large avascular tissue, it requires a unique transport system that delivers nutrients and removes waste products from the lens centre (Mathias et al., 1997). This system is thought to be generated by the metabolically active differentiating lens fibre cells (DF) that contain mitochondria and utilise aerobic metabolism, and the lens epithelial cells that contain active Na^+/K^+ ATPases. These outer cells perform active transport that generates circulating ionic and fluid fluxes that deliver nutrients and antioxidants to the mature fibre cells (MF) via an extracellular route. MF cells lack mitochondria and other cellular organelles, and therefore utilise anaerobic metabolism to provide their energy requirements (Mathias et al., 1997). The primary fibres are laid down *in utero* and must remain transparent for the entire lifetime of the organism. They are connected to the surface cells by gap junction channels which provide a pathway for the outflow of ions and water towards the Na^+/K^+ ATPases located in the metabolically more active cells at the lens surface.

Perturbation of this system is thought to lead to age-related nuclear (ARN) cataract formation, which is the major cause of blindness worldwide. In particular, the lens antioxidant glutathione (GSH) is central to lens redox balance and long term protein homeostasis, and an age-related decrease in its nuclear concentration (Harding, 1970; Lou et al., 1990; Sweeney and Truscott, 1998), reduces the protective mechanisms used by MF cells to guard against oxidative stress, leading to protein aggregation and opacification (Fig. 1) (Lou, 2003; Lou et al., 1990; Lou et al., 1986; Truscott, 2005). In the bovine lens GSH concentration reaches ~8μmol/g in the outer cortex, and ~1 μmol/g in the nucleus (Lim et al., 2016). The high concentration in the outer cortex is maintained via a combination of GSH

uptake, *de novo* synthesis from its precursor amino acids (cysteine, glutamate and glycine) and GSH regeneration from glutathione disulfide (GSSG), the oxidised form of GSH, via NADPH-based reduction. With advancing age, a barrier to the movement of GSH forms in the lens, causing GSH levels to fall abruptly in the central lens nucleus relative to the outer cortical fibres, thereby exposing the nucleus of the lens to the damaging effects of reactive oxygen species (ROS), which ultimately leads to ARN cataract. The redox balance of specific lens regions is clearly important to normal lens function, yet our knowledge of how the location and relative abundance of metabolites that contribute to antioxidant defence systems of the lens is limited.

Through its reactive thiol group, GSH interacts with many other small molecules and metabolites, and therefore functions not only to maintain intracellular redox balance and to reduce peroxides and free radicals in the lens, but in many other cellular processes. Such processes include the maintenance of protein structure and function by reducing the disulfide linkages of proteins, the regulation of protein synthesis and degradation, and the detoxification of reactive chemicals and endogenous metabolites (Wang and Ballatori, 1998). For example GSH is central to the glyoxalase system, which detoxifies methylglyoxal and other reactive aldehydes that are produced as part of normal metabolism. Methylglyoxal, which can be formed through lipid peroxidation and glycolysis, is highly cytotoxic, and is thought to be involved in the formation of advanced glycation end products (AGEs) (Mannervik, 2008) that modify lens proteins and can lead to cataract formation in diabetics (Nagaraj et al., 2012).

Hyperbaric oxygen (HBO) therapy has been used to treat decompression sickness, embolisms, and promote healing of poorly vascularised wounds, however since the documentation of the elevated rate of cataract occurrence in patients after HBO therapy, nuclear cataract has been recognised as a contraindication (Palmquist et al., 1984). This is because molecular oxygen can traverse fibre cell membranes and cytoplasm to reach the nucleus, promoting ROS formation and compromising redox balance throughout the lens. Since this link to cataract was described, HBO has been used as an experimental tool to investigate the process of ARN cataractogenesis. *In vivo* exposure of guinea pigs to HBO increases lens light scatter, depletes nuclear GSH and water soluble protein, and increases lipid peroxidation (Giblin et al., 1995). Decreased GSH content and water-soluble proteins were seen in the *in vitro* HBO treated rabbit lens (Giblin et al., 1988; Padgaonkar et al., 2000). Guinea pigs exposed to 3 atm oxygen for 5.5 hours exhibited cell loss and pyknosis in both the corneal endothelium and lens epithelium, two tissues that are in direct contact with aqueous humour-borne oxygen (Nichols et al., 1972). In the bovine lens HBO accelerates the appearance of physiological symptoms of lens aging. Biochemical assays have revealed a decreased GSH:GSSG ratio and elevated levels of oxidative stress markers and lens protein glutathionylation (Cappiello et al., 1995; Lim et al., 2016). Fifteen-hour exposure to HBO induces changes to lens refractive index and optical power, while five-hour exposure is sufficient to induce changes to GSH and GSSG concentrations (Lim et al., 2016). Quantitative data therefore exist, however spatial information remains limited to comparing nuclear and cortical homogenates. Given that the initial step in the mode of action of HBO is ROS generation, which affects metabolic antioxidants before crystallin proteins and optical function, in this study we have identified and spatially localized changes

to GSH metabolism in response to oxidative stress by comparing the distribution of GSH metabolites in the normal and HBO treated lens. We chose a five hour HBO exposure to capture the initial metabolic changes associated with lens aging. To do this in a spatially-resolved way, we have utilised MALDI mass spectrometry profiling and imaging approaches.

The ability of imaging mass spectrometry (IMS) to spatially map many analytes in a single dataset make it ideal for an exploration of GSH-related metabolites in the lens. While MALDI-IMS has been used extensively to study lens proteins (Anderson et al., 2015; Grey et al., 2009; Grey and Schey, 2009; Wenke et al., 2015) and lipids (Pol et al., 2015; Vidová et al., 2010), IMS of lens metabolites is limited (Grey, 2016). We therefore utilised high dynamic range (HDR) mass spectrometry with the continuous accumulation of selected ions (CASI) to detect metabolites in lens regions with maximum sensitivity (Spraggins et al., 2012), LC-MS/MS to confirm metabolite identities, and MALDI FTICR IMS to spatially localise glutathione and its metabolites throughout bovine lens sections. We show that while glutathione-related metabolic intermediates involved in detoxification pathways remained relatively unchanged in response to oxidative stress, compounds involved in its antioxidant function were altered.

2. MATERIALS AND METHODS

2.1 Tissue and Reagents

All reagents were purchased from Sigma-Aldrich (St Louis, MO). Bovine eyes were sourced from the local abattoir, and lenses removed from the eyes anteriorly. Lenses were either frozen immediately and stored at −80 °C until required for cryosectioning, or placed in the tissue culture fluid Medium 199 at 37 °C to maintain lens homeostasis during hyperbaric chamber treatment.

2.2 Hyperbaric chamber treatment

Bovine lenses in Medium 199 at 37 °C were incubated for 5 hrs in a hyperbaric chamber (Parr Instrument Company, Moline, IL) with 100% O_2 at 100 atm to induce oxidative stress. As a control for hyperbaric treatment, N_2 was substituted for O_2 in a separate set of experiments. Following hyperbaric treatment, all lenses were immediately frozen and stored at −80 °C until required.

2.3 Tissue sectioning and preparation

Frozen lenses were mounted on cold chucks using OCT compound (Tissue-Tek, Sakura Finetek, Torrances CA) at the base of the tissue only. 20μm axial sections were cut using a cryostat (Leica CM3050S, Leica Microsystems GmbH, Wetzlar, Germany), and collected on to room temperature MALDI targets using methanol landing, which maintains lens tissue section integrity on MALDI plates (Han and Schey, 2006). Tissue was then placed in a vacuum desiccator for 30 mins prior to matrix application. 9-aminoacridine (9AA) was applied to the tissue sections using a custom-built vacuum sublimation apparatus. Briefly, a vacuum of 50 mTorr was applied to the tissue, and the chamber heated to 160 °C for 12 min, while cooling the sample plate with ice/water slurry. Approximate matrix density applied

was 100 μg/cm^2. Following matrix deposition, prepared MALDI plates were subjected to rehydration with 80% EtOH. Briefly, the MALDI plate was attached to the inside of a glass Petri dish lid with copper tape. The lid was placed in an oven set at 85 °C for 1 min, then placed on the Petri dish base which contained filter paper wet with 100 μl of 80% EtOH. The dish was sealed and placed in the oven for a further 2 min, before removing and opening the dish to allow it to dry. Rehydrated samples were then placed in a vacuum desiccator until data collection.

2.4 High Dynamic Range-MALDI mass spectrometry

High Dynamic Range (HDR)-MALDI mass spectrometry was carried out using a 9.4T Bruker solariX ESI/MALDI FTICR mass spectrometer (Bruker Daltonics, Billerica, MA) (Spraggins et al., 2012). HDR-MALDI mass spectra were collected in the range *m/z* 200 to 1600 in negative ion mode from cortex and nucleus regions of control and treated bovine lens sections. Continuous accumulation of selected ions (CASI) was utilised to increase sensitivity. HDR-MALDI data was collected using a CASI window of 100 mass units, and scanning the centre mass in 50 Da steps to cover the entire mass range. For each CASI spectrum, 10 000 laser shots were accumulated. By using the quadrupole mass filter to limit the mass range, CASI significantly increases the effective sensitivity by maximizing the ion population from the selected mass range. All CASI spectra that constituted one HDR-MALDI mass spectrum were collected in 15 mins, and no signal degradation was detected during sampling. Each CASI spectrum collected across the full mass range were exported as a generic text file format, then combined to produce a full HDR-MALDI spectrum using Microsoft Excel, before being imported into mMass (Strohalm et al., 2008) for baseline subtraction, smoothing and peak picking. Finally, peak lists generated from mMass were used to interrogate the Metlin metabolomics database (Scripps Center for Metabolomics, La Jolla, CA) for putative identifications based on mass accuracy (<5 ppm).

2.5 MALDI Imaging mass spectrometry

MALDI imaging was carried out using a 9.4T Bruker solariX ESI/MALDI FTICR mass spectrometer (Bruker Daltonics, Billerica, MA) using flexImaging v3.0. MALDI imaging data sets collected in negative ion mode from *m/z* 300 – 1000, with a spatial resolution of 150 μm. Sections from control and treated lenses were analysed in the same image so that relative intensity levels of detected analytes could be compared directly between samples. Identification of signals detected in the MALDI FTICR IMS datasets were made using accurate mass assignment (<5 ppm) and fragmentation data collected using LC-MS/MS of microdissected bovine lens regions with an Orbitrap mass analyser (Q-Exactive, Thermo Fisher Scientific, Waltham, MA) (see methods below). MALDI images were assembled using flexImaging v3.0. Data sets were normalised to RMS intensity and MALDI images plotted at the observed *m/z* ± 0.001 Da, with pixel interpolation on. Three full imaging datasets (fresh, HBO and HBN lenses) were collected from three separate hyperbaric chamber experiments. MALDI images from one representative dataset are presented.

2.6 LC-MS/MS identification of glutathione conjugates

Frozen bovine lenses were thawed in a Petri dish at room temperature. During this process the outer 50% of the lens volume was removed with tweezers and placed in a

microcentrifuge tube (cortex) and the remaining lens tissue placed in a separate microcentrifuge tube (nucleus). Each fraction was homogenised using a micropestle. Extraction of small molecules and metabolites was performed by addition of 700µl of 60% methanol to each lens fraction followed by incubation at 4°C for 16 hours. Samples were then centrifuged at 15 000 RPM for 90 minutes at 4°C (Eppendorf 5415R), and 500µl of the supernatants collected and filtered through a 3kDa MWCO centrifugal filter (Amicon Ultra, 0.5ml) for 50 minutes at 15 000 RPM (Eppendorf 5415R) to remove proteins and peptides. The 500µl aliquots were then lyophilised using a SpeedVac (Thermo Fisher Scientific, Waltham, MA) and resuspended in 20µl of 50%ACN/5mM ammonium acetate. UHPLC-MS/MS was conducted using an Accela 1250 pump coupled to a Q-Exactive Orbitrap mass spectrometer (Thermo Fisher Scientific, Waltham, MA) operating in heated electrospray ionisation mode. Chromatographic separations were performed using a Syncronis C18 100 × 2.1 mm, 1.7µm column (Thermo Fisher Scientific, Waltham, MA). Solvent A and B were 0.1% formic acid in water and 0.1% formic acid in acetonitrile, respectively. A flow rate of 0.40 ml min^{-1} was applied with a gradient elution profile: 95% B for 2 minutes, ramped to 99% A for 12.5 minutes, followed by a 10 minute hold at 99% A before a rapid return to 95% B over 1 minute and re-equilibrated there for 10 minutes. Centroid MS scans were acquired in the mass range of *m/z* 285 – 750 using the Orbitrap mass spectrometer with mass resolution of 35 000 (FWHM as defined at *m/z* 200) in negative ion mode. An inclusion list was used to target glutathione conjugates putatively identified by accurate mass using the MALDI imaging data. Qual Browser software (Xcalibur v2.2, Thermo Fisher Scientific, Waltham, MA) was used to manually compare acquired tandem mass spectra of glutathione conjugates with reference mass spectra from the Metlin metabolomics database (Scripps Center for Metabolomics, La Jolla, CA).

3. RESULTS

3.1 MALDI FTICR mass spectrometry for spatially-resolved lens metabolomics

Since the lens contains both nucleated, metabolically and transcriptionally active fibre cells, and terminally differentiated central lens fibre cells, the level of cellular metabolism in a lens fibre cell is dependent on its location, age, and differentiation state. In order to investigate changes in lens fibre cell metabolites in the normal lens and in ARN cataract formation, a spatially-resolved technique is ultimately required. However, as an initial step we performed HDR-MALDI FTICR mass spectrometry tissue profiling (Spraggins et al., 2012), which allowed us to analyse cortical and nuclear regions of normal lenses and lenses exposed to hyperbaric oxygen (HBO) or nitrogen (HBN) as a control. In this analysis, spatial resolution is sacrificed in order to maximise sensitivity of the mass spectrometer, allowing detection of many more metabolites than with ‘traditional’ full-scan MALDI FTICR mass spectrometry and identification by accurate mass measurement (Table 1). Since this analysis detected a variety of glutathione-related metabolites and glutathione is known to play a central role in ARN cataract formation, our subsequent analysis to spatially localize metabolites using MALDI IMS (Caprioli et al., 1997) focussed on glutathione and related metabolites. Identifications of ions detected in the MALDI datasets were assigned based on accurate mass measurements and LC-MS/MS analysis of microdissected lens region extracts was used to confirm assigned identities where possible. In the results presented below, axial lens

sections were oriented with the anterior pole to the left, however, no anterior-posterior spatial differences were observed for the detected metabolites.

3.2 Metabolite screening of lens regions with HDR-MALDI FTICR Mass Spectrometry

Using HDR-MALDI FTICR mass spectrometry, thousands of discrete *m/z* signals were detected in each region from each lens section (Table 1). When metabolomics databases were interrogated with each list of *m/z* peaks, the identities of the majority of the *m/z* peaks were unknown. However, hundreds of peaks from each list were putatively identified and the list was subsequently manually inspected and reduced based on known experimental parameters such as species, likely exposure to xenobiotics, etc, to increase confidence in the putative identifications. Putative lipid and peptide matches were also excluded in order to focus on non-lipid metabolites. The refined number of putatively identified lens metabolites is shown in Table 1 and the full list is included in Supplemental Information.

A variety of metabolite classes that included fatty acids, nucleosides, nucleotides, sugars and their derivatives, and antioxidants were detected in each lens region. For example, the nucleotide ATP, which is known to be found in the lens in high concentrations (Greiner et al., 1985) and is both an energy molecule and purinergic signalling molecule in the lens (Eldred et al., 2003), was detected in cortex and nucleus regions of all lens sections, while other less abundant nucleotides such as IMP and XMP were also detected in some lens regions (see Supplemental Information). Interestingly, nitrotyrosine, which is considered a marker of cell damage and can be produced under oxidative stress, was only detected in the HBO-treated lens sections, indicating that the metabolome of these lenses had indeed been altered by HBO treatment. Previously, nitrotyrosine levels have been shown to be reduced with N-acetyl cysteine (Martinez et al., 2015), a precursor to glutathione that was also detected in the HDR-MALDI analysis. What was striking from the HDR-MALDI data was the number of glutathione conjugates detected in each lens section. For example, twelve discrete glutathione conjugates were detected in the normal bovine lens cortex alone. Since the HDR-MALDI FTICR MS was not collected in a quantitative way and has limited spatial fidelity, MALDI FTICR IMS was applied to sister sections from each lens to map the spatial distribution and relative concentration of lens metabolites at higher spatial resolution. Glutathione conjugates were focussed on specifically (Table 2) due to the high number and variety that were detected in the HDR-MALDI analysis and to the important roles that GSH is known to play in lens homeostasis and ARN cataract formation.

3.3 Glutathione and reducing equivalents

An ion detected at *m/z* 306.0763 was identified as the reduced form of glutathione (0.65 ppm). GSH was detected throughout the normal bovine lens, and was most abundant in the lens cortex, and decreased in the lens nucleus (Fig. 2, *top row, left*). An identical distribution of GSH was detected in the HBN-treated lenses, indicating that the GSH concentration and distribution was unaffected by treatment with an inert gas at high pressure, or organ culture (Fig. 2, *top row, middle*). However, in HBO treated lenses, GSH signal was not detected in the lens nucleus, and became restricted to the lens periphery (Fig. 2, *top row, right*). Similarly, an ion detected at *m/z* 611.1446 and identified as glutathione disulfide (GSSG, 0.16 ppm), the oxidised form of glutathione, was detected in the lens cortex of normal and

HBN-treated control lenses (Fig. 2, *middle row, left* and *middle*). Following HBO treatment, GSSG abundance increased in the lens periphery and became restricted to this lens region (Fig. 2, *middle row, right*). The ion in the mass spectrum at *m/z* 744.0831 was assigned NADPH (0.94 ppm), which helps to regenerate GSH from GSSG in a reaction catalysed by glutathione reductase. NADPH was also found in cortical regions of the normal and HBN-treated lenses (Fig. 2, *bottom row, left* and *middle*), but was restricted to the lens periphery in HBO-treated lenses (Fig. 2, *bottom row, right*). [Note that these metabolites were detected in the nucleus of normal lenses by the more sensitive HDR-MALDI profiling].

3.4 Glutathione in detoxification

An ion detected at *m/z* 378.0977 was assigned S-Lactoylglutathione (0.26 ppm). S-Lactoylglutathione is an intermediate metabolite formed in the detoxification of the highly cytotoxic methylglyoxal, a metabolic by-product of glycolysis. Methylglyoxal is the precursor to several known AGEs that are implicated in diabetic complications such as cortical cataract. One of the main detoxification mechanisms of methylglyoxal is by the glyoxalase system, a two-step enzymatic process which is present and active in the lens (Haik Jr et al., 1994) (Fig. 3A). Since the glyoxalase system is dependent upon the availability of GSH, oxidative stress can severely limit its effectiveness. In the normal lens, S-lactoylglutathione was most abundant in the outer cortex; in the same region that GSH is most abundant (Fig. 3B). However, HBO treatment did not appear to affect the abundance or distribution of S-lactoylglutathione.

Formaldehyde (HCHO) is a widely distributed (Kalasz, 2003) cellular metabolite that reacts rapidly to cross-link a variety of biomacromolecules and small molecules. It is generated through cellular processes such as (Slater, 1984) and N-demethylation of various endogenous and exogenous compounds *in situ* (Kalasz, 2003). Therefore, the regulation of intra- and extracellular HCHO levels is critical to normal cell function, and occurs via an enzyme-catalysed reaction utilising GSH (Fig. 4A). Low levels of each intermediate in HCHO detoxification were detected in the outer cortex of normal lenses. Upon HBO treatment, the levels of an ion detected at *m/z* 336.0873 and assigned S-hydroxymethylglutathione (0.60 ppm) appeared unchanged (Fig. 4B), while an ion detected at *m/z* 334.0715 and assigned S-formylglutathione (0.30 ppm) was slightly decreased (Fig. 4C).

3.5 Other endogenous glutathione conjugates

An ion detected at *m/z* 425.0807 was identified as cysteine-glutathione disulfide (CySSG, 0.24 ppm), which is formed endogenously through a thiol-disulfide exchange reaction between GSH and L-cystine (Fig. 5A) (Eriksson and Eriksson, 1967). While it is found throughout the body, CySSG was localised to the inner cortex of normal bovine lenses (Fig. 5B, *left*), and was largely absent in lenses treated with HBO (Fig. 5B, *right*).

S-(1,2-Dicarboxyethyl)glutathione is a GSH conjugate formed from the reaction between GSH and L-malate (Fig. 6A), which is an intermediate in the citric acid cycle. It has previously been found in the rat liver, heart and the lens in considerable amounts, and in some systems has shown an anti-inflammatory effect (Sakaue et al., 1996). An ion detected

at *m/z* 422.0874 and assigned S-(1,2-Dicarboxyethyl)glutathione (0.24 ppm) was predominantly localized in the outer cortex of normal lenses (Fig. 6B). Upon HBO treatment, its distribution remained cortical, but its abundance was increased.

A notable output from the emerging field of polysulfidomics (Toohey and Cooper, 2014) is the abundance of polysulfur compounds in the human body. Cysteine persulfides (CySSH) appear at >100μM in the mouse brain, and 50μM in other tissues (Ida et al., 2014), and are produced by enzymes that have also been found in the lens (Persa et al., 2006; Persa et al., 2004). CySSH and other persulfides can then undergo polysulfide exchange reactions with other thiol containing compounds to yield per- and poly-sulfides. Since GSH is the most abundant thiol compound in the lens, CySSH would be expected to react with GSH to form glutathione persulfide, also known as S-sulfanylglutathione, which can itself act as an antioxidant. The high GSH concentrations in the lens suggest higher concentrations of S-sulfanylglutathione would also be expected (Everett and Wardman, 1995). In our MALDI imaging analysis of bovine lenses, an ion detected at *m/z* 338.0487 was assigned S-sulfanylglutathione (0.30 ppm), and was localised to the cortex of normal and HBN lenses (Fig. 7B, *left* and *middle*, respectively). Upon HBO treatment, the signal intensity for S-sulfanylglutathione was unchanged, while its distribution was reminiscent of the distribution of GSH (see Fig. 2), being restricted to more peripheral lens fibre cells than the control lenses.

4. DISCUSSION

In this study we report the presence, relative abundance and distribution of GSH and its endogenous conjugates in the normal bovine lens and in a model of lens aging. GSH conjugates involved in detoxification of reactive metabolites remained relatively unchanged in the aging lens model, while metabolites involved in its antioxidant function were altered following HBO treatment (Table 3). It is likely that many of the observed glutathione conjugates are involved in multiple metabolic pathways and lens cell functions. While in the following discussion we interpret the observed HBO-induced changes in glutathione conjugate distributions with regards to current literature, the physiology of metabolites that are newly described in the lens deserves further attention.

Using the MALDI FTICR imaging approach, most GSH conjugates were localised to the lens cortex, which was predicted since this region of the lens contains more metabolically active lens cells. For example, reduced and oxidised forms of glutathione were detected in the cortical regions of the normal lens and in the HBO-treated lenses. However, no signal was detected in the HBO lens nucleus, despite the confirmed presence of these molecules in the lens nucleus using other techniques (Giblin et al., 1988; Lou et al., 1990; Sweeney and Truscott, 1998) and in the HDR-MALDI FTICR MS data presented here (Supplemental Table 1). While this could be due to the ionisation of these metabolites being suppressed by the local environment, the fact that they were detected using HDR-MALDI MS suggests that these metabolites are at concentrations in the lens nucleus below the detection limit of the mass spectrometer when operating in full-scan imaging mode. The development of an imaging methodology with enhanced sensitivity is the goal of future experiments, and may be achieved through modulation of the mode of operation of the mass spectrometer, through

on-tissue chemical derivatisation of target metabolites to enhance their ionisation efficiency, or through the use of alternative MALDI matrices. Nevertheless, we observed a reduction in the spatial distribution and signal level of GSH, and an increase in the signal level of GSSG in the lens cortex following HBO treatment that is consistent with results using alternative techniques from similar experimental procedures (Giblin et al., 1988). Together these results indicate that HBO treatment of bovine lenses, an experimental approach that has been validated biochemically and optically as a model for lens aging (Lim et al., 2016), elicits metabolic changes detectable by MALDI mass spectrometry that are associated with aging and ARN cataract formation.

The endogenous GSH conjugate that changed the most dramatically after HBO treatment was cysteine-glutathione disulfide. CySSG, which is suggested to be a storage form of L-cysteine, showed a highly localised distribution in normal bovine lens inner cortex which was largely absent in lenses treated with HBO (see Fig. 5). This suggests that the oxidative insult contributes to the degradation of CySSG. While it is possible that enzymatic reduction of CySSG could liberate free L-cysteine (Pihl et al., 1957) (Eriksson and Mannervik. 1970), we did not detect free L-cysteine since the collected mass range did not include the predicted *m/z* of L-cysteine. Since previous analyses have shown protein-thiol mixed disulfide formation is increased following HBO treatment (Giblin et al., 1995; Lim et al., 2016), it is likely that the dramatic decrease in CySSG signal in the HBO lens inner cortex is contributing to their formation. Further investigation of the distribution of free L-cysteine in HBO-treated lenses to investigate these hypotheses is ongoing.

S-(1,2-dicarboxyethyl)glutathione is typically found in the lens in considerable amounts (Calam and Waley, 1963). In the present study, it was detected in the cortex of normal and control lenses, and its abundance increased following HBO treatment, presumably due to an increase in either L-malate or fumarate, which are substrates for GSH-dependent formation of S-(1,2-dicarboxyethyl)glutathione (Tsuboi et al., 1990). Malate (Wu et al., 2008) and S-(1,2-dicarboxyethyl)glutathione have been suggested to support redox balance in rat heart and liver. Since malate is a product of the citric acid cycle it is likely to be abundant in a molecular oxygen-rich environment such as the cortex during HBO treatment. The role of S-(1,2-dicarboxyethyl)glutathione has been investigated in cataract formation in galactose-fed rats (Tsuboi et al., 1984) and naphthalene-treated rabbits (Takemura et al., 1996), where it was proposed as a potential anti-cataract compound since its levels declined with formation of initial opacities, but recovered in lenses that recovered transparency. Our results suggest an increase in S-(1,2-dicarboxyethyl)glutathione in response to a cataractogenic insult, which is in contrast to the galactose- and naphthalene-induced cataracts. This could be due to the timeframe over which the experiment was performed. Lenses were treated for 5 hours with HBO, which may be too short a time to detect a decrease in S-(1,2-dicarboxyethyl)glutathione, or the detected increase in S-(1,2-dicarboxyethyl)glutathione signal intensity could be due to a transient increase in its concentration in response to the oxidative insult. Alternatively, this unexpected increase could be due to different metabolic effects manifested in the galactose/naphthalene-induced cataract model and the HBO model of lens aging. Finally, the accumulation of S-(1,2-dicarboxyethyl)glutathione could be due to a functional decrease of glutathione conjugate transporters (OATPs and MRPs) that have been shown to mediate glutathione conjugate efflux in the rat lens (Umapathy et al., 2013),

although it is not known whether the same transporters are present in the bovine lens and whether their function is affected by HBO treatment. Clearly the role of S-(1,2-dicarboxyethyl)glutathione in normal lens function and cataract formation is complex and warrants further investigation.

In the present study, two intermediate metabolites involved in formaldehyde detoxification were detected in the lens cortex, S-hydroxymethylglutathione, and S-formylglutathione. While formaldehyde is likely present in all cells as a result of normal cellular metabolism, it is also a common product of lipid peroxidation which occurs through lipid interaction with molecular oxygen. Therefore, the detection of elevated levels of each formaldeyde detoxification intermediate was predicted after treatment of lenses with HBO. There was minimal change in the level of S-hydroxymethylglutathione, and a small decrease in the level of S-formylglutathione, which is not consistent with upregulation of the formaldehyde detoxification system. It is possible that the incubation of the lens in HBO was not long enough to detect a marked upregulation of these metabolic intermediates, or that the activity of the transporters responsible for export of these specific GSH conjugates was sufficient to respond to their elevated concentration, thus exporting them effectively and maintaining normal tissue levels of these GSH conjugates.

Similarly, no change in the relative abundance or distribution of S-lactoylglutathione, the intermediate in methylglyoxal detoxification, was seen following HBO treatment. The main source of methylglyoxal is glycolysis which is not targeted by our HBO model of lens aging. Furthermore the appearance of methylglyoxal-AGEs on lens proteins correlate with lens opacification and brunescence, though it is likely these reactions occur over years rather than hours (Shamsi et al., 1998), hence the constant distribution of S-lactoylglutathione in Fig. 3.

HBO-induced changes to S-sulfanylglutathione distributions were reminiscent of GSH (compare Figs 2 and 7), disappearing from the inner cortex and nuclear regions while slightly increasing in the outermost cortex. This observation would suggest an antioxidant function for S-sulfanylglutathione similar to GSH. Indeed, Ida et al (2014) demonstrate the enzymatic production of CySSH and its role in forming per- and poly-sulfide compounds that have enhanced antioxidant function. The enzymes cystathionase and cystathionine beta-synthase, which have been found in the lens and are induced by oxidative stress (Persa et al 2004), were shown to directly produce CySSH, which can then conduct polysulfur exchange with GSH to yield S-sulfanylglutathione. Glutathione persulfides are stronger reductants than glutathione (Massey et al., 1971), are found at 50–100 μM in mammalian organs, and when oxidised can be reduced by glutathione reductase (Ida et al., 2014). The similarities between Figs 2 and 7 lend weight to S-sulfanylglutathione having an antioxidant function (Everett and Wardman, 1995) and being relevant to lens redox balance. Overall, the relative stability of GSH conjugates involved in detoxification in the HBO model supports the notion that ARN cataract formation subsequent to a decrease in GSH levels is more likely due to the role of GSH as an antioxidant than as a detoxification molecule.

5. CONCLUSIONS

In summary, high sensitivity and mass resolution mass spectrometry techniques have been used to detect and image the key lens antioxidant, GSH, and its endogenous conjugates directly from ocular lens tissue sections. Furthermore, this approach detected changes in metabolic intermediates involved in the antioxidant and detoxification functions of GSH in a model of lens aging. Glutathione conjugates were detected that increased, decreased, or remained unchanged in HBO-treated lenses. This study highlights the multifunctional role of GSH in the lens, and provides insight into the metabolic changes that take place in ARN cataract.

Supplementary Material

Refer to Web version on PubMed Central for supplementary material.

Acknowledgments

The authors wish to acknowledge the support of grants from the NIH/NIGMS (2 P41 GM103391-06) and the National Institutes of Health Shared Instrumentation Grant Program (1S10OD012359-01) awarded to RMC. The authors also acknowledge the support of the Health Research Council of New Zealand, the Marsden Fund of New Zealand, and the Auckland Medical Research Foundation.

Abbreviations

MALDI	matrix-assisted laser desorption/ionisation
IMS	imaging mass spectrometry
HDR	high dynamic range
FTICR	Fourier transform ion cyclotron resonance
GSH	reduced glutathione
GSSG	oxidised glutathione
CySSG	cysteine-glutathione disulfide
CySSH	cysteine persulfide
NADPH	nicotinamide dinucleotide phosphate (reduced)

REFERENCES

Anderson DM, Floyd KA, Barnes S, Clark JM, Clark JI, McHaourab H, Schey KL. A method to prevent protein delocalization in imaging mass spectrometry of non-adherent tissues: application to small vertebrate lens imaging. Anal. Bioanal. Chem. 2015; 407:2311–2320. [PubMed: 25665708]

Bassnett S. The fate of the Golgi apparatus and the endoplasmic reticulum during lens fiber cell differentiation. Invest. Ophthalmol. Vis. Sci. 1995; 36:1793–1803. [PubMed: 7635654]

Bassnett S, Beebe DC. Coincident loss of mitochondria and nuclei during lens fiber cell differentiation. Dev. Dyn. 1992; 194:85–93. [PubMed: 1421526]

Calam DH, Waley SG. Acidic peptides of the lens 8. S-(αß-dicarboxyethyl) glutathione. Biochem. J. 1963; 86:226–231. [PubMed: 14017790]

Cappiello M, Vilardo PG, Cecconi I, Leverenz V, Giblin FJ, Del Corso A, Mura U. Occurrence of glutathione-modified aldose reductase in oxidatively stressed bovine lens. Biochem. Biophys. Res. Commun. 1995; 207:775–782. [PubMed: 7864872]

Caprioli RM, Farmer TB, Gile J. Molecular Imaging of Biological Samples: Localization of Peptides and Proteins Using MALDI-TOF MS. Anal. Chem. 1997; 69:4751–4760. [PubMed: 9406525]

Eldred JA, Sanderson J, Wormstone M, Reddan JR, Duncan G. Stress-induced ATP release from and growth modulation of human lens and retinal pigment epithelial cells. Biochem. Soc. Trans. 2003; 31:1213–1215. [PubMed: 14641028]

Eriksson B, Eriksson SA. Synthesis and characterization of the L-cysteine-glutathione mixed disulfide. Acta Chem. Scand. 1967; 21:1304–1312. [PubMed: 6051513]

Eriksson SA, Mannervik B. The reduction of the L-cysteine-glutathione mixed disulfide in rat liver involvement of an enzyme catalyzing thiol-disulfide interchange. FEBS Lett. 1970; 7:26–28. [PubMed: 11947421]

Everett SA, Wardman P. Perthiols as antioxidants: radical-scavenging and prooxidative mechanisms. Methods Enzymol. 1995; 251:55–69. [PubMed: 7651231]

Giblin FJ, Padgaonkar VA, Leverenz VR, Lin LR, Lou MF, Unakar NJ, Dang L, Dickerson JE Jr, Reddy VN. Nuclear light scattering, disulfide formation and membrane damage in lenses of older guinea pigs treated with hyperbaric oxygen. Exp. Eye Res. 1995; 60:219–235. [PubMed: 7789403]

Giblin FJ, Schrimscher L, Chakrapani B, Reddy VN. Exposure of rabbit lens to hyperbaric oxygen in vitro: regional effects on GSH level. Invest. Ophthalmol. Vis. Sci. 1988; 29:1312–1319. [PubMed: 3417415]

Greiner JV, Kopp SJ, Glonek T. Distribution of phosphatic metabolites in the crystalline lens. Invest. Ophthalmol. Vis. Sci. 1985; 26:537–544. [PubMed: 3980170]

Grey AC. MALDI imaging of the eye: Mapping lipid, protein and metabolite distributions in aging and ocular disease. International Journal of Mass Spectrometry. 2016; 401:31–38.

Grey AC, Chaurand P, Caprioli RM, Schey KL. MALDI imaging mass spectrometry of integral membrane proteins from ocular lens and retinal tissue. J. Proteome Res. 2009; 8:3278–3283. [PubMed: 19326924]

Grey AC, Schey KL. Age-related changes in the spatial distribution of human lens a-crystallin products by MALDI imaging mass spectrometry. Invest. Ophthalmol. Vis. Sci. 2009; 50:4319–4329. [PubMed: 19387068]

Haik GM Jr, Lo TWC, Thornalley PJ. Methylglyoxal Concentration and Glyoxalase Activities in the Human Lens. Exp. Eye Res. 1994; 59:497–500. [PubMed: 7859825]

Han J, Schey KL. MALDI tissue imaging of ocular lens alpha-crystallin. Invest. Ophthalmol. Vis. Sci. 2006; 47:2990–2996. [PubMed: 16799044]

Harding JJ. Free and protein-bound glutathione in normal and cataractous human lenses. Biochem. J. 1970; 117:957–960. [PubMed: 5451916]

Ida T, Sawa T, Ihara H, Tsuchiya Y, Watanabe Y, Kumagai Y, Suematsu M, Motohashi H, Fujii S, Matsunaga T, Yamamoto M, Ono K, Devarie-Baez NO, Xian M, Fukuto JM, Akaike T. Reactive cysteine persulfides and S-polythiolation regulate oxidative stress and redox signaling. Proc. Natl. Acad. Sci. U. S. A. 2014; 111:7606–7611. [PubMed: 24733942]

Kalasz H. Biological role of formaldehyde, and cycles related to methylation, demethylation, and formaldehyde production. Mini Rev. Med. Chem. 2003; 3:175–192. [PubMed: 12570834]

Lim JC, Vaghefi E, Li B, Nye-Wood MG, Donaldson P. Characterization of the effects of hyperbaric oxygen on the biochemical and optical properties of the bovine lens. Invest. Ophthalmol. Vis. Sci. 2016; 57:1961–1973. [PubMed: 27096754]

Lou MF. Redox regulation in the lens. Progress in retinal and eye research. 2003; 22:657–682. [PubMed: 12892645]

Lou MF, Dickerson JE Jr, Garadi R. The role of protein thiol mixed disulfides in cataratogenesis. Exp. Eye Res. 1990; 50:819–826. [PubMed: 2373174]

Lou MF, McKellar R, Chyan O. Quantitation of lens protein mixed disulfides by ion-exchange chromatography. Experimental eye research. 1986; 42:607–616. [PubMed: 3720875]

Mannervik B. Molecular enzymology of the glyoxalase system. Drug Metabol. Drug Interact. 2008; 23:13–27. [PubMed: 18533362]

Martinez PF, Bonomo C, Guizoni DM, Junior SA, Damatto RL, Cezar MD, Lima AR, Pagan LU, Seiva FR, Fernandes DC, Laurindo FR, Novelli EL, Matsubara LS, Zornoff LA, Okoshi K, Okoshi MP. Influence of N- acetylcysteine on oxidative stress in slow-twitch soleus muscle of heart failure rats. Cell. Physiol. Biochem. 2015; 35:148–159. [PubMed: 25591758]

Massey V, Williams CH Jr, Palmer G. The presence of S degrees-containing impurities in commercial samples of oxidized glutathione and their catalytic effect on the reduction of cytochrome c. Biochem. Biophys. Res. Commun. 1971; 42:730–738. [PubMed: 5543955]

Mathias RT, Rae JL, Baldo GJ. Physiological properties of the normal lens. Physiol. Rev. 1997; 77:21–50. [PubMed: 9016299]

Nagaraj RH, Linetsky M, Stit AW. The pathogenic role of Maillard reaction in the aging eye. Amino Acids. 2012; 42:1205–1220. [PubMed: 20963455]

Nichols CW, Yanoff M, Hall DA, Lambertsen CJ. Histologic alterations produced in the eye by oxygen at high pressure. Arch. Ophthalmol. 1972; 87:417–421. [PubMed: 5018246]

Padgaonkar VA, Leverenz VR, Fowler KE, Reddy VN, Giblin FJ. The effects of hyperbaric oxygen on the crystallins of cultured rabbit lenses: a possible catalytic role for copper. Exp. Eye Res. 2000; 71:371–383. [PubMed: 10995558]

Palmquist BM, Philipson B, Barr PO. Nuclear cataract and myopia during hyperbaric oxygen therapy. Br. J. Ophthalmol. 1984; 68:113–117. [PubMed: 6691953]

Persa C, Osmotherly K, Chen KC-W, Moon S, Lou MF. The distribution of cystathionine β-synthase (CBS) in the eye: implication of the presence of a trans-sulfuration pathway for oxidative stress defense. Experimental eye research. 2006; 83:817–823. [PubMed: 16769053]

Persa C, Pierce A, Ma Z, Kabil O, Lou M. The presence of a transsulfuration pathway in the lens: a new oxidative stress defense system. Experimental eye research. 2004; 79:875–886. [PubMed: 15642325]

Pihl A, Eldjarn L, Bremer J. On the mode of action of X-ray protective agents III. The enzymatic reduction of disulfides. J. Biol. Chem. 1957; 227:339–345. [PubMed: 13449077]

Pol J, Faltyskova H, Krasny L, Volny M, Vlacil O, Hajduch M, Lemr K, Havlicek V. Age-related changes in the lateral lipid distribution in a human lens described by mass spectrometry imaging. Eur J Mass Spectrom. 2015; 21:297–303.

Sakaue T, Matsumoto S, Tsuboi S, Ogata K, Ohmori S. Protective effect of S-(1,2-dicarboxyethyl)glutathione, an intrinsic tripeptide in liver, heart and lens, and its esters on acetaminophen-induced hepatotoxicity in rats. Biol. Pharm. Bull. 1996; 19:1216–1219. [PubMed: 8889044]

Shamsi FA, Lin K, Sady C, Nagaraj RH. Methylglyoxal-derived modifications in lens aging and cataract formation. Invest. Ophthalmol. Vis. Sci. 1998; 39:2355–2364. [PubMed: 9804144]

Slater TF. Free-radical mechanisms in tissue injury. Biochem. J. 1984; 222:1–15. [PubMed: 6383353]

Spraggins, JM., Grove, K., Cornett, DS., Caprioli, RM. Massively Enhanced Sensitivity and Dynamic Range for Molecular Imaging using High Dynamic Range (HDR) - MALDI FT-ICR MS. 60th ASMS Annual Conference; Vancouver, Canada. 2012.

Strohalm M, Hassman M, Košata B, Kodíček M. mMass data miner: an open source alternative for mass spectrometric data analysis. Rapid Commun. Mass Spectrom. 2008; 22:905–908. [PubMed: 18293430]

Sweeney MHJ, Truscott RJW. An impediment to glutathione diffusion in older normal human lenses: a possible precondition for nuclear cataract. Exp. Eye Res. 1998; 67:587–595. [PubMed: 9878221]

Takemura M, Ueno H, Kodama H. S-(1,2-dicarboxyethyl)glutathione and Glutathione in Lens and Liver of Naphthalene-Treated Rabbits. Eur. J. Clin. Chem. Clin. Biochem. 1996; 34:85–90. [PubMed: 8833638]

Toohey JI, Cooper AJ. Thiosulfoxide (sulfane) sulfur: new chemistry and new regulatory roles in biology. Molecules. 2014; 19:12789–12813. [PubMed: 25153879]

Truscott RJ. Age-related nuclear cataract-oxidation is the key. Exp. Eye Res. 2005; 80:709–725. [PubMed: 15862178]

Tsuboi S, Kobayashi M, Nanba M, Imaoka S, Ohmori S. S-(1,2-dicarboxyethyl)glutathione and activity for its synthesis in rat tissues. J Biochem. 1990; 107:539–545. [PubMed: 2358427]

Tsuboi S, Uda N, Ikeda M, Hirota K, Ohmori S. S-(1,2-dicarboxyethyl)glutathione and S-(1,2-dicarboxyethyl) L-cysteine in lens. J. Clin. Chem. Clin. Biochem. 1984; 22:285–290. [PubMed: 6547471]

Umapathy A, Donaldson P, Lim J. Antioxidant delivery pathways in the anterior eye. Biomed Res Int. 2013; 207250:26.

Vidová V, Pól J, Volný M, Novák P, Havlíček V, Wiedmer SK, Holopainen JM. Visualizing spatial lipid distribution in porcine lens by MALDI imaging high-resolution mass spectrometry. J. Lipid Res. 2010; 51:2295–2302. [PubMed: 20388918]

Wang W, Ballatori N. Endogenous Glutathione Conjugates: Occurrence and Biological Functions. Pharmacol. Rev. 1998; 50:335–356. [PubMed: 9755286]

Wenke JL, Rose KL, Spraggins JM, Schey KL. MALDI Imaging Mass Spectrometry Spatially Maps Age-Related Deamidation and Truncation of Human Lens Aquaporin-0. Invest. Ophthalmol. Vis. Sci. 2015; 56:7398–7405. [PubMed: 26574799]

Wu JL, Wu QP, Yang XF, Wei MK, Zhang JM, Huang Q, Zhou XY. L-malate reverses oxidative stress and antioxidative defenses in liver and heart of aged rats. Physiol. Res. 2008; 57:261–268. [PubMed: 17298203]

Highlights

- Bovine lens glutathione distribution is mapped using MALDI imaging mass spectrometry
- Reduced glutathione is less concentrated following hyperbaric oxygen exposure
- Multiple lens glutathione conjugate distributions are presented
- Effects of lens hyperbaric oxygen exposure on glutathione conjugates are shown

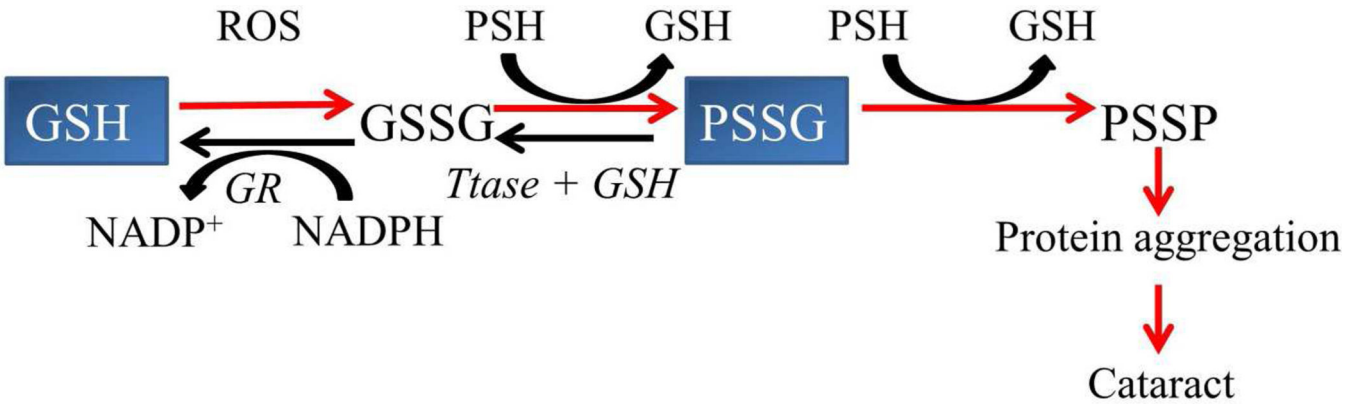

Fig. 1. Role of glutathione in lens cataract formation

Schematic diagram of the role of glutathione in protection of lens proteins from oxidative damage. GSH can neutralise reactive oxygen species (ROS) directly, and form GSSG as a result. GSH can be regenerated by glutathione reductase (GR) and the coenzyme NADPH. If GSH is depleted, protein mixed disulfides can form (PSSG), leading to protein cross-linking (PSSP), protein aggregation and lens opacification. Adapted from Lou et al (2003).

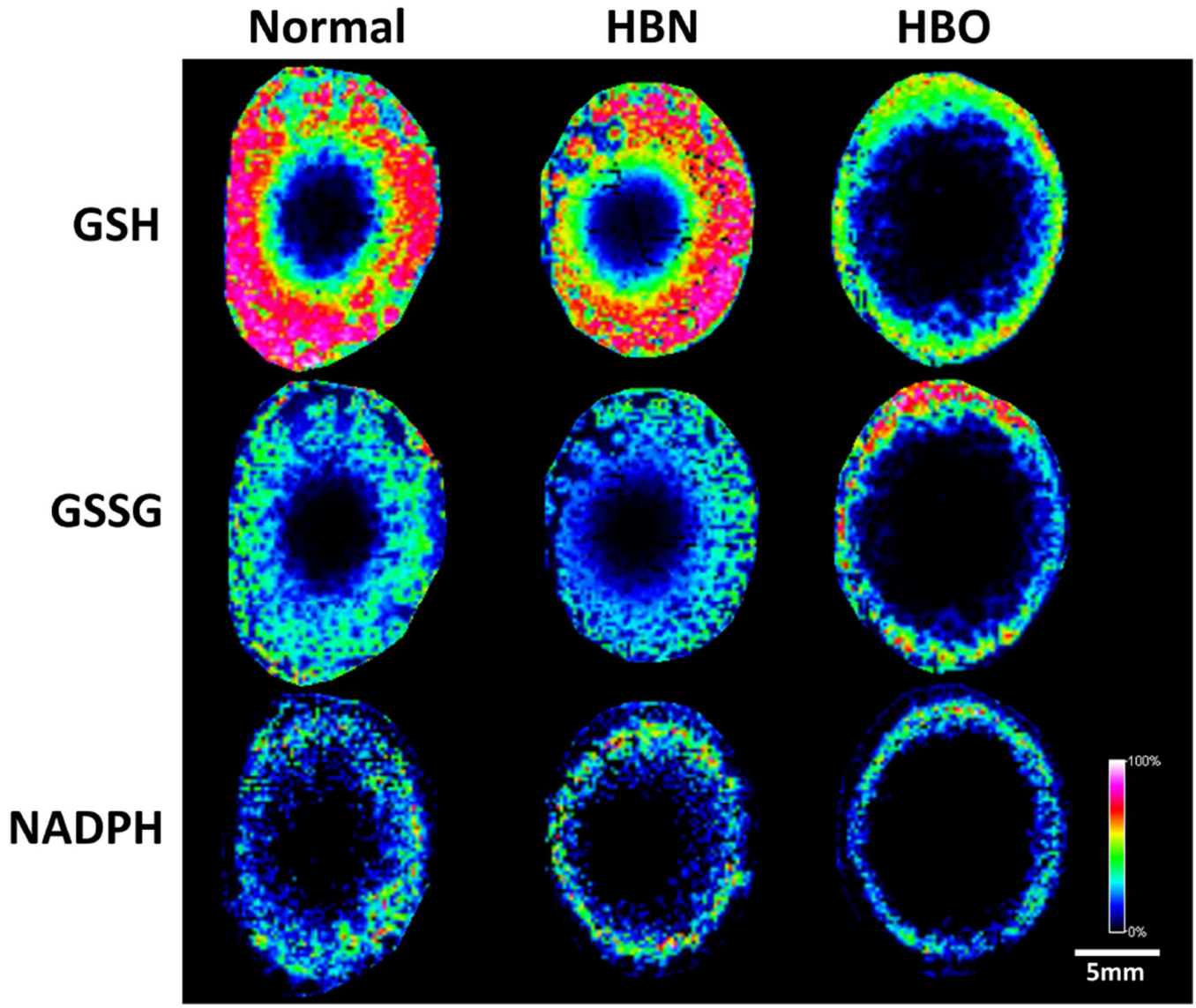

Fig. 2. Spatial distributions of GSH, GSSG and NADPH

MALDI FTICR images of reduced glutathione (GSH, *top*), oxidised glutathione (GSSG, *middle*) and reduced nicotinamide adenine dinucleotide phosphate (NADPH, *bottom*) in normal (*left*), hyperbaric nitrogen-treated (HBN, *middle*) and hyperbaric oxygen-treated (HBO, *right*) axial bovine lens sections collected at 150 μm spatial resolution.

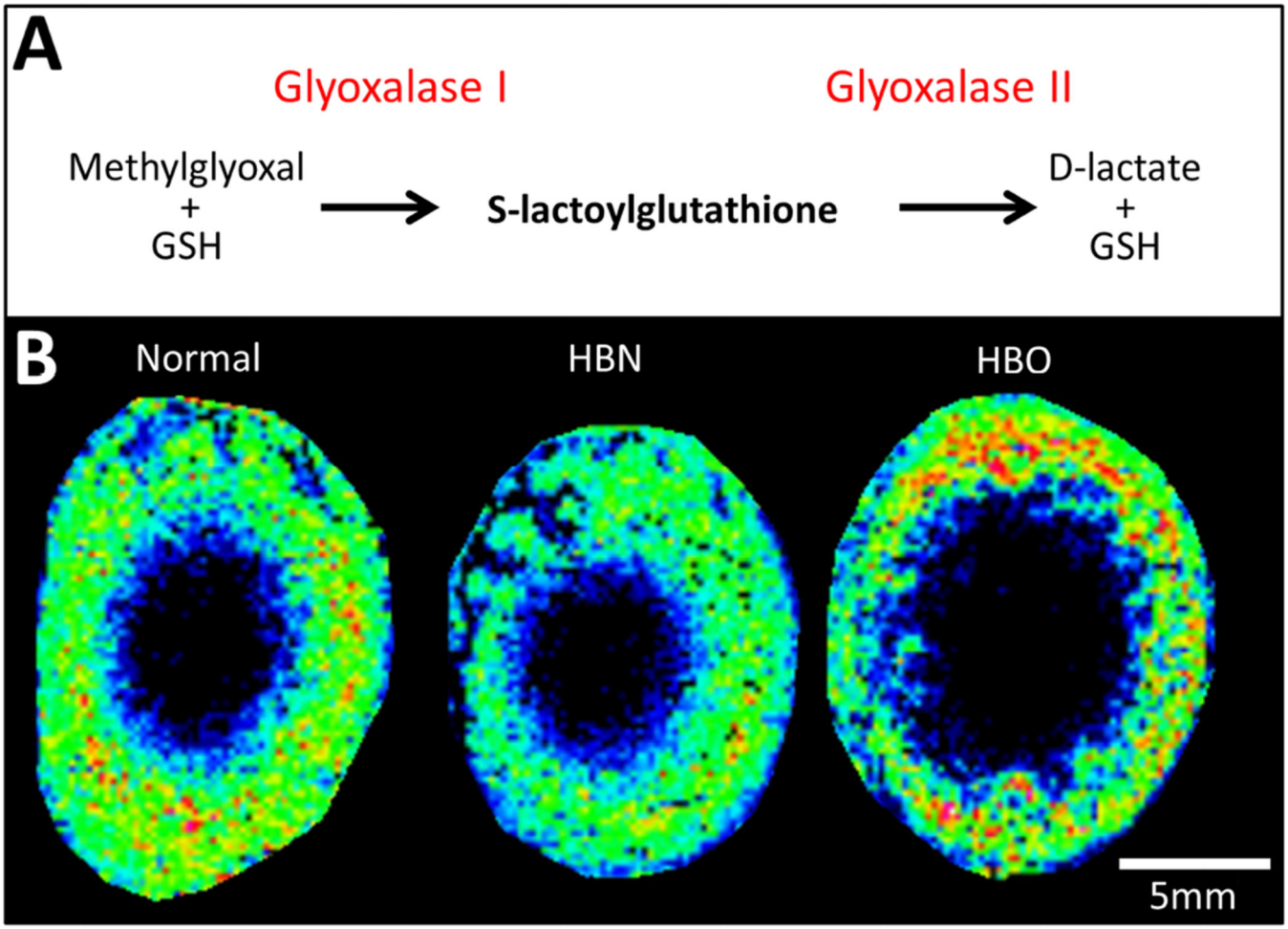

Fig. 3. Spatial distribution of intermediate of methylglyoxal detoxification

(A) Schematic diagram of the glyoxalase system to detoxify methylglyoxal via interaction with GSH. Enzymes are shown in red, bold text indicates metabolite detected in MALDI images. (B) MALDI FTICR images of the distribution of S-lactoylglutathione in normal (*left*), HBN- (*middle*), and HBO-treated (*right*) axial bovine lens sections.

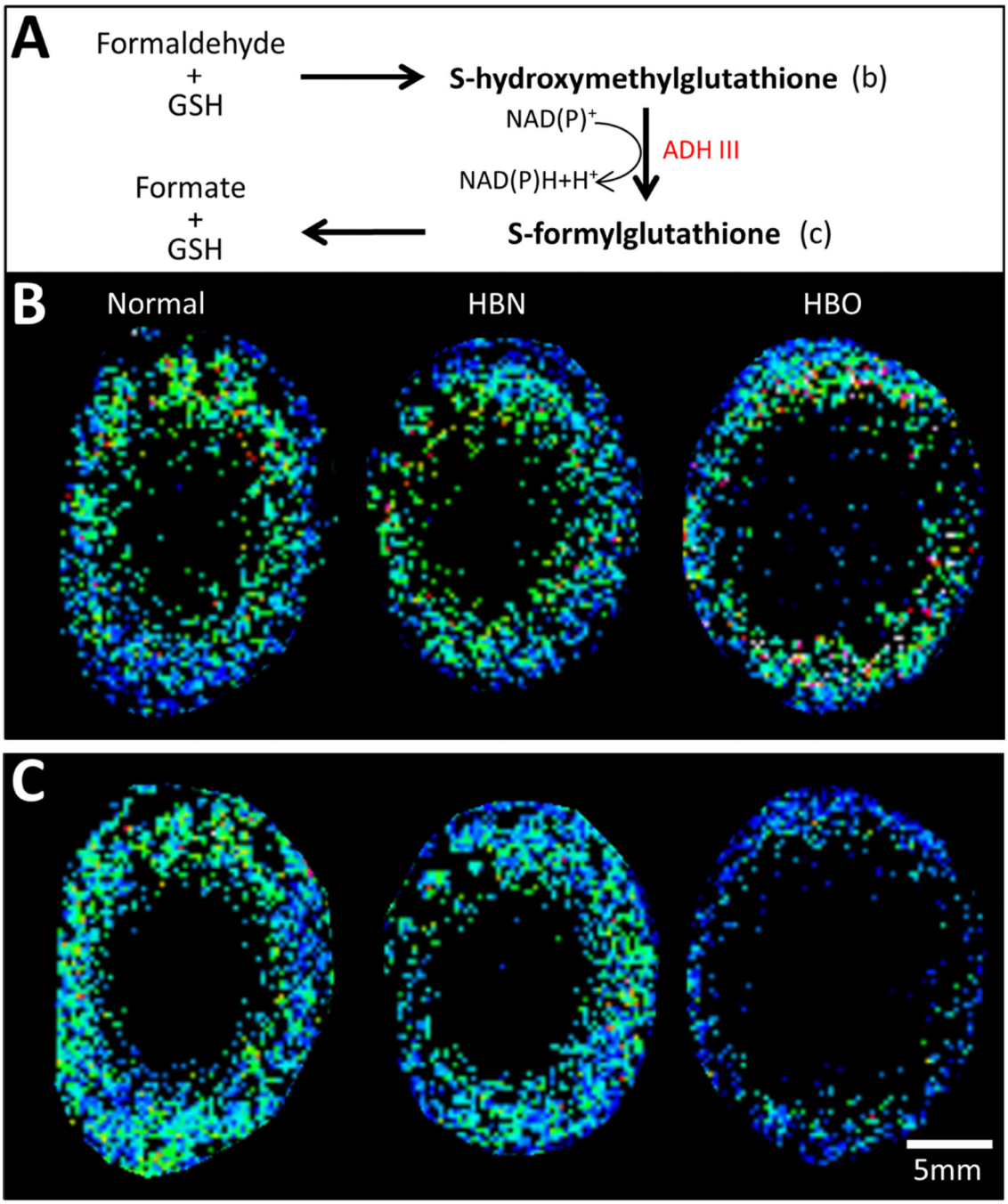

Fig. 4. Spatial distributions of intermediates in formaldehyde detoxification

(A) Schematic diagram of the detoxification of cellular formaldehyde to formate via interaction with GSH. The spatial distributions of the two glutathione conjugates (*bold text*) in this pathway, S-hydroxymethylglutathione and S-formylglutathione, are shown in (B) and (C), respectively, of normal, HBN- and HBO-treated bovine lenses.

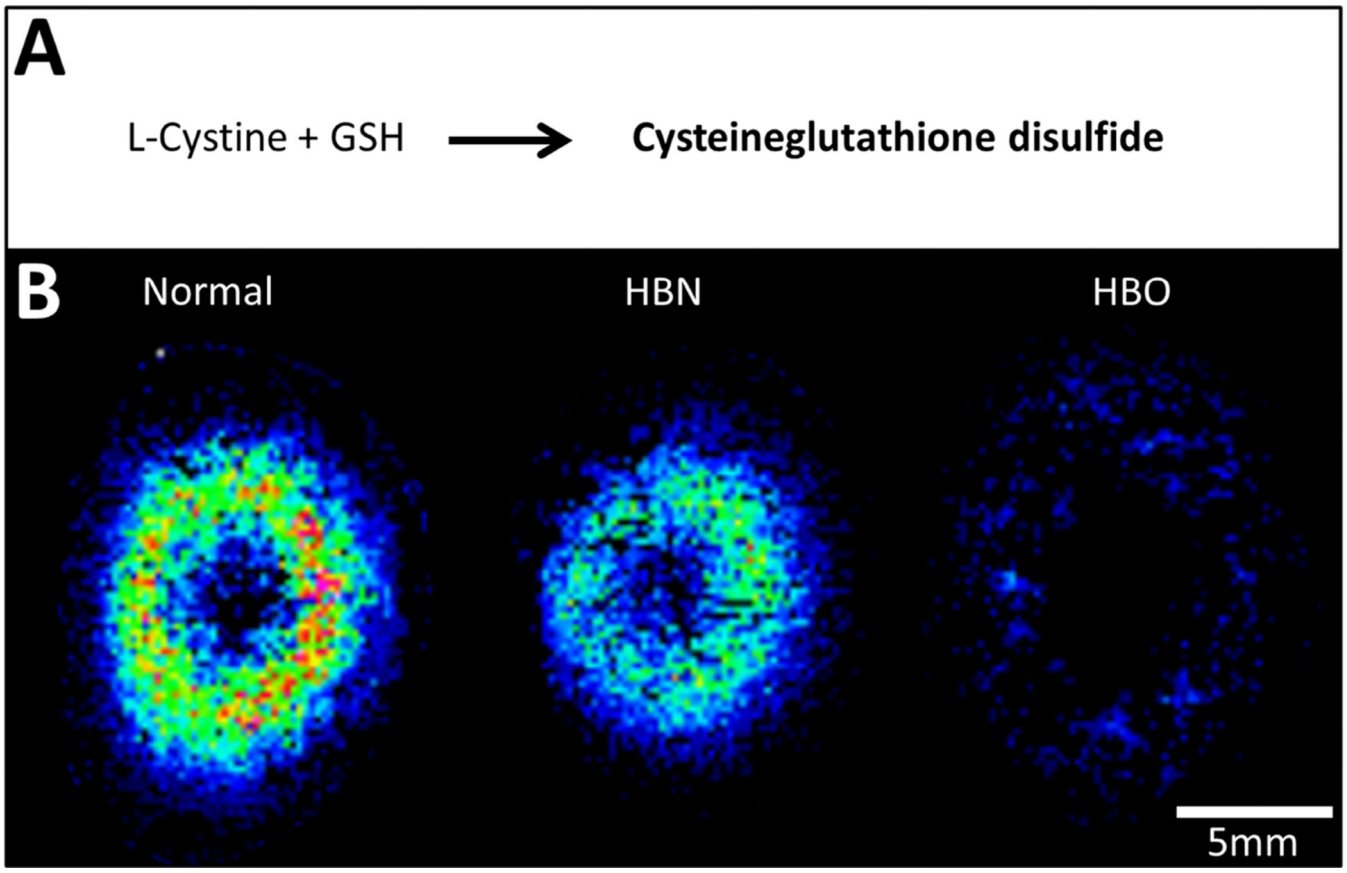

Fig. 5. Spatial distribution of cysteine-glutathione disulfide

(A) Schematic diagram of the formation of cysteine-glutathione disulfide. (B) MALDI FTICR image of cysteine-glutathione distribution in axial sections from normal, HBN- and HBO-treated lenses.

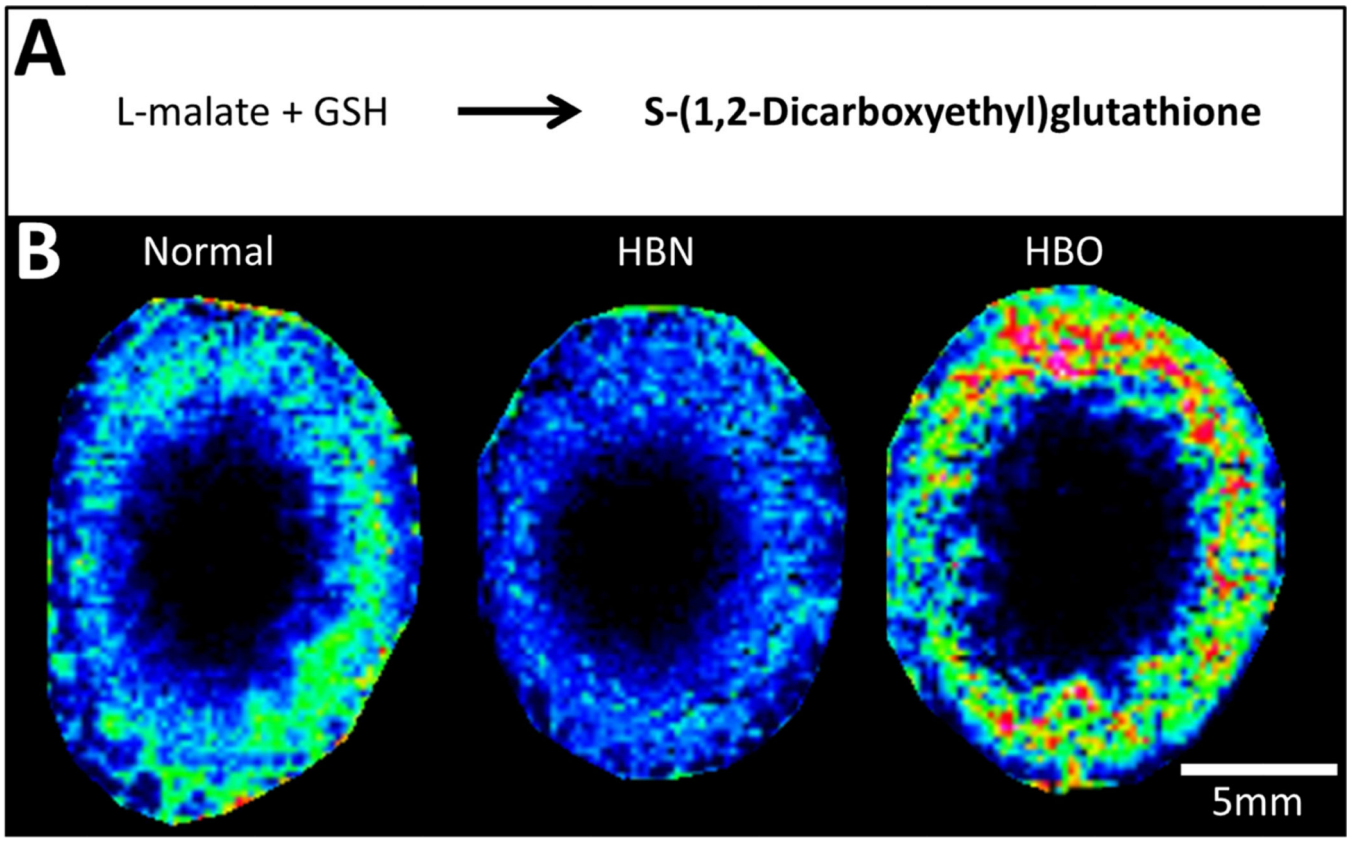

Fig. 6. Spatial distribution of S-(1,2-dicarboxyethyl)glutathione in bovine lenses

(A) Schematic diagram of the formation of S-(1,2-dicarboxyethyl)glutathione. (B) MALDI FTICR image of the distribution of S-(1,2-dicarboxyethyl)glutathione in axial sections from normal, HBN- and HBO-treated bovine lenses.

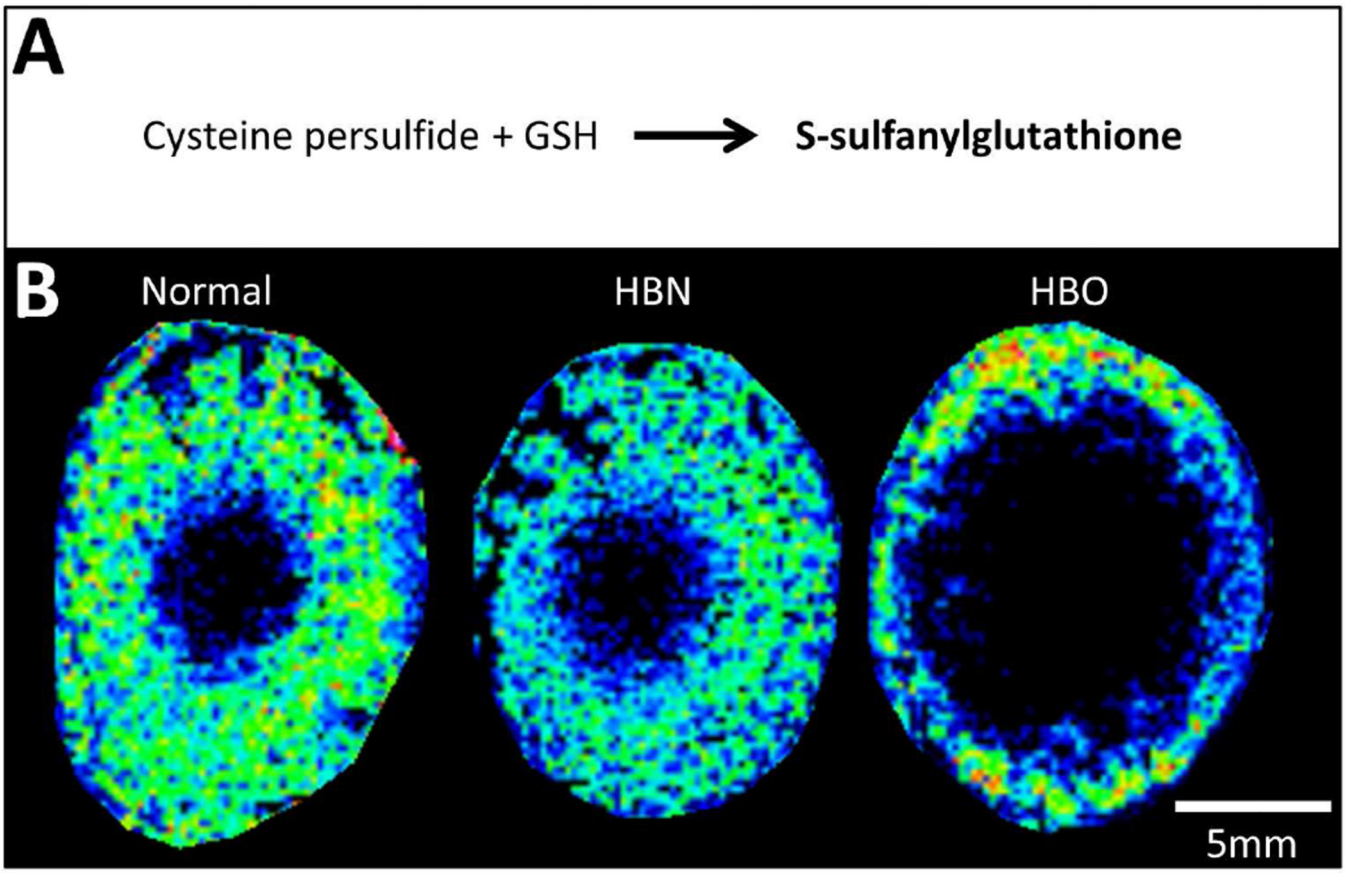

Fig. 7. Spatial distribution of S-sulfanylglutathione in bovine lenses

(A) Schematic diagram of the formation of S-sulfanylglutathione by disulfide exchange with cysteine persulfide. (B) MALDI FTICR image of the distribution of S-sulfanylglutathione in axial sections from normal, HBN- and HBO-treated bovine lenses.

Table 1

Numbers of lens small molecule *m/z* signals detected from HDR MALDI mass spectrometry experiment

Class of m/z signals	Normal Cortex	Normal Nucleus	HBN Cortex	HBN Nucleus	HBO Cortex	HBO Nucleus
All (non-deisotoped)	4170	3572	2616	2116	2253	2614
Putatively identified from database matching	136	146	136	129	158	156
Glutathione and conjugates	12	12	12	11	14	14

Exp Eye Res. Author manuscript; available in PMC 2018 January 01.

Table 2

Predicted and observed *m/z* for glutathione-related metabolites detected by MALDI imaging, all identities confirmed by LC-MS/MS

Molecule	Predicted m/z $[M-H]^-$	Observed m/z $[M-H]^-$	Error (ppm)
Glutathione (GSH)	306.0765	306.0763	0.65
Glutathione disulfide (GSSG)	611.1447	611.1446	0.16
Cysteine-glutathione disulfide (CySSG)	425.0806	425.0807	0.24
S-formylglutathione	334.0714	334.0715	0.30
S-(hydroxymethyl)glutathione	336.0871	336.0873	0.60
S-Lactoylglutathione	378.0976	378.0977	0.26
S-(1,2-dicarboxyethyl)glutathione	422.0875	422.0874	0.24
S-sulfanylglutathione	338.0486	338.0487	0.30
Nicotinamide adenine dinucleotide phosphate (NADPH)	744.0838	744.0831	0.94

Table 3

Summary of glutathione-related metabolite distributions in HBN- and HBO-treated bovine lenses mapped by MALDI imaging

Molecule	HBN			HBO		
	OC	IC	N	OC	IC	N
Glutathione (GSH)	✓	✓	✓	✓	✓	X
Glutathione disulfide (GSSG)	✓	✓	X	✓	X	X
Cysteine-glutathione disulfide (CySSG)	X	✓	X	X	✓	X
S-formylglutathione	✓	✓	X	✓	✓	X
S-(hydroxymethyl)glutathione	✓	✓	X	✓	✓	X
S-Lactoylglutathione	✓	✓	X	✓	✓	X
S-(1,2-dicarboxyethyl)glutathione	✓	✓	X	✓	✓	X
S-sulfanylglutathione	✓	✓	X	✓	X	X
Nicotinamide adenine dinucleotide phosphate (NADPH)	✓	✓	X	✓	X	X